

Computer Assisted EPID Analysis of Breast Intrafractional and Interfractional Positioning Error

Jason W. Sohn*, David B. Mansur[†], James I. Monroe*, Robert E. Drzymala[‡],
Hosang Jin[‡], Taesuk Suh[§], James F. Dempsey[‡], Eric E. Klein[†]

*Department of Radiation Oncology, Ireland Cancer Center, Case Western Reserve University School of Medicine, Cleveland, [†]Department of Radiation Oncology, Mallinckrodt Institute of Radiology, Washington University School of Medicine, St. Louis, [‡]Department of Radiation Oncology, University of Florida College of Medicine, Gainesville, [§]Department of Biomedical Engineering, Kangnam St. Mary's Hospital, Korea

Automated analysis software was developed to measure the magnitude of the intrafractional and interfractional errors during breast radiation treatments. Error analysis results are important for determining suitable planning target volumes (PTV) prior to implementing breast-conserving 3-D conformal radiation treatment (CRT). The electrical portal imaging device (EPID) used for this study was a Portal Vision LC250 liquid-filled ionization detector (fast frame-averaging mode, 1.4 frames per second, 256×256 pixels). Twelve patients were imaged for a minimum of 7 treatment days. During each treatment day, an average of 8 to 9 images per field were acquired (dose rate of 400 MU/minute). We developed automated image analysis software to quantitatively analyze 2,931 images (encompassing 720 measurements). Standard deviations (σ) of intrafractional (breathing motion) and interfractional (setup uncertainty) errors were calculated. The PTV margin to include the clinical target volume (CTV) with 95% confidence level was calculated as $2 \cdot (1.96 \cdot \sigma)$. To compensate for intrafractional error (mainly due to breathing motion) the required PTV margin ranged from 2 mm to 4 mm. However, PTV margins compensating for interfractional error ranged from 7 mm to 31 mm. The total average error observed for 12 patients was 17 mm. The interfractional setup error ranged from 2 to 15 times larger than intrafractional errors associated with breathing motion. Prior to 3-D conformal radiation treatment or IMRT breast treatment, the magnitude of setup errors must be measured and properly incorporated into the PTV. To reduce large PTVs for breast IMRT or 3-D CRT, an image-guided system would be extremely valuable, if not required. EPID systems should incorporate automated analysis software as described in this report to process and take advantage of the large numbers of EPID images available for error analysis which will help individual clinics arrive at an appropriate PTV for their practice. Such systems can also provide valuable patient monitoring information with minimal effort.

Key Words : Electronic portal image device, Breast, Canny edge detection, Radiation treatment, Positional error

INTRODUCTION

Planning Target Volumes (PTV) as described in the International Commission on Radiation Units and Measurements (ICRU) Report 50¹⁾ are designed to compensate for factors that prevent the accurate treatment of the Clinical Target

Volume (CTV). Sources of errors are generally broken down into three categories: anatomical mobility (i.e. breathing motion), anatomical variations (i.e. mobile breast tissue), and external factors (i.e. patient setup errors, beam geometries). The PTV is expressed as an expansion of the CTV volume by adding a 'margin' for a particular type of treatment. The determination of this margin is critical for successful treatment. If the margin is too small, portions of the CTV are likely not to receive a therapeutic dose. A PTV volume that is too large will propagate excess irradiation of normal tissue. To determine an appropriate PTV margin an analysis of contributing factors should be performed at each institution. It is sometimes easier to address errors by separating them accord-

Submitted March 14, 2006, accepted March 22, 2006.

Corresponding Author: Jason W. Sohn, Department of Radiation Oncology, Ireland Cancer Center, Case Western Reserve University School of Medicine, Cleveland, OH 44106-6068.

Tel: 216-844-2736, Fax: 216-844-2005

E-mail: Jason.sohn@uhhs.com

ing to their frequency of occurrence: i.e., Intrafractional (during irradiation) and Interfractional (between radiation sessions). Interfractional setup error is the main contributor to the size of the PTV margin.²⁾ Tissue deformation and mobility originate from the inherent characteristics of breast tissue and hence also contribute to interfractional error. Intrafractional error is the positional error incurred during a daily treatment fraction. Breathing and/or voluntary patient movement may cause this positional change.

Breast radiation treatments initially brought up many concerns regarding positional uncertainties resulting from breathing motion and setup error. There is extensive literature reporting on positional error and its dosimetric consequences.²⁻⁹⁾ Among these studies, EPIDs were the most common tools used to measure the magnitude of the breathing and interfractional setup error. EPIDs are offered in a variety of imaging methods, which include the single and cine imaging modes. Single mode can acquire an image before, during, and after a treatment. Cine imaging mode takes multiple images during a treatment, providing information of patient positioning during a treatment fraction. EPIDs come with image-analyzing and operating software. However, tools provided with the software normally only handle single image analysis. Therefore, it is currently cumbersome and laborious to analyze the large number of images needed to accurately determine patient positional errors on a routine clinical basis.

Measurements involved in analyzing images are often performed by tracking the tissue-and-air and/or lung-and-chestwall interfaces. For individual image analysis, the distance was measured from the beam edge to one of those interfaces. Since these interfaces form very steep image-intensity gradients, we investigated the use of an edge detection algorithm as the basis for an analysis tool. There are many well-known edge/interface-detecting algorithms including: Canny, Nalwa-Binford, Sarkar-Boyer, and Sobel.¹⁰⁻¹³⁾ Among the edge detection algorithms proposed so far, the Canny edge detection algorithm is the most robustly defined operator and is widely used. The popularity of the Canny edge detection algorithm based on three criteria: good detection, localization, and single response to a step edge.^{14,15)}

We investigated the intrafractional and interfractional positional error by creating an automated analysis software pack-

age designed to process large numbers of EPID images. Our study goals were to develop and evaluate automated EPID analysis software to learn how accurately breast patients were positioned, and to use the results for determining PTV margins.

MATERIALS AND METHODS

1. Patient treatment position and geometry

Patients were positioned in alpha cradles with the ipsilateral arm over the head holding a bar attached to the alpha cradle. Custom alpha cradles were made for each patient, which extended from above the head to the patient's waist. They were scanned for treatment planning using a large bore CT simulator (AcQSim, Philips, Cleveland, OH). The orthogonal setup marks were placed along with tangential field's borderlines. During the treatment planning process, 2-D custom compensator filters¹⁶⁾ were generated using a commercial treatment planning system (Focus, Computerized Medical System, St. Louis, MO) for all patients to achieve uniform dose distribution. All patients were instructed to breathe normally during CT scanning and treatments. Twelve patients participated in this study. Five of the 12 patients were treated to the right breast, and the remaining patients were treated to the left breast. The gantry angles used for treatments are summarized in Fig. 1 and Fig. 2. All of these patients were treated with 2 fields, tangential beams only. None of them had the supraclavicular, axillary, or internal mammary nodes treated with separate fields.

2. Acquisition of EPID images

While treating patients, electronic portal images were taken with a commercial EPID (PortalVision-LC250, Varian, Palo Alto, CA). As shown in Fig. 3, images exhibited the checkerboard pattern due to the use of 2-D custom compensator filters fabricated with aluminum and copper cubes mounted on a Perspex tray. The EPID utilizes arrays of liquid-filled ionization chambers. It was set to run in a fast frame-averaging mode with an image acquisition rate of 1.4 frames/second. All treatments were delivered at a 400 MU/min dose rate. For each patient an average of 8 images per field were acquired during a treatment. This image acquisition was

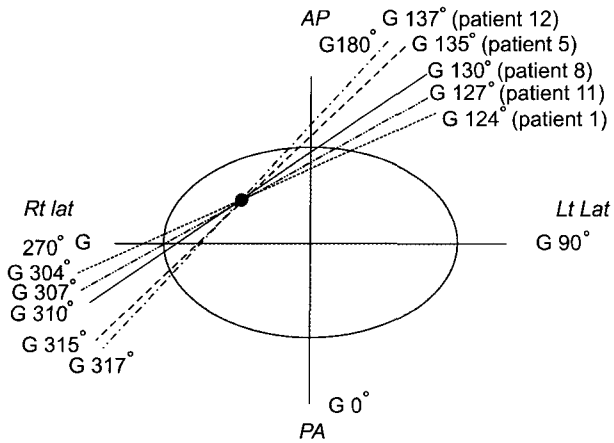


Fig. 1. Five patients had right breast treatment. The medial and lateral gantry angles ranged from 124° to 137° and from 304° to 317° respectively.

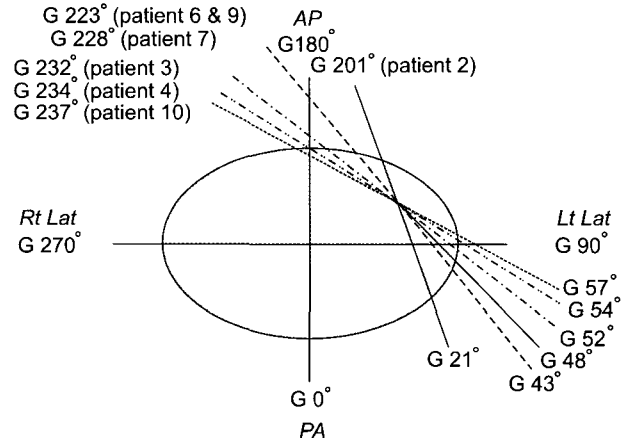


Fig. 2. Seven patients had left breast treatment. The lateral and medial gantry angles ranged from 21° to 57° and from 201° to 237° respectively.

repeated for a minimum of 7 treatment days. Each patient had approximately 240 images for tangential fields. All fields were defined with multi-leaf collimators (1 cm leaf width).

3. Automated analysis software

A custom software package was developed using a commercial data analysis and programming software package (Matlab®, Mathworks). The custom software is composed of three modules: (1) compressed Varian formatted image files are imported and uncompressed, (2) tissue edge detection and automated line drawing along the tissue edge, and (3) geometric measurement and statistical analysis. The Canny method was used to detect the tissue interfaces and to locate the edge of the breast tissue.^{10,14,15)} This method finds edges by identifying local maxima of the gradient of image intensities. Pixels are classified as an edge if the gradient magnitude of the pixel is larger than those of pixels at both sides in the direction of maximum intensity change. The typical implementation of the Canny edge detection algorithm involves 4 steps. First, the Canny algorithm smooths the image with a Gaussian filter to reduce the sharpness of the image details. Second, it determines gradient magnitude and gradient direction at each pixel. If the gradient magnitude at a pixel is larger than those at its two neighbors in the gradient direction, it marks the pixel as an edge. Otherwise, the pixel is marked as part of the background. Finally, the Canny system removes the weak edges by hysteresis thresholding¹⁴⁾ where

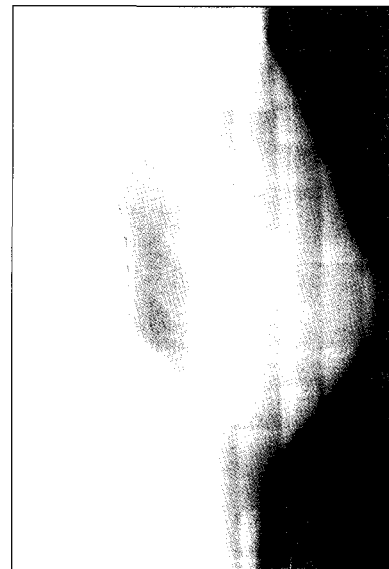


Fig. 3. A sample electronic portal image taken during radiation treatments using an EPID employing arrays of liquid-filled ionization chambers.

weak edges below a low threshold are eliminated, but not if they are connected to an edge above a high threshold. The Canny edge detection algorithm was implemented as a built-in function in the Matlab® imaging toolbox. Our experience has shown the Canny method can be one of the best edge-detection algorithms for electronic portal image analysis.

Edge detection was performed on each acquired image to trace field edges and tissue interfaces such as lung-tissue and

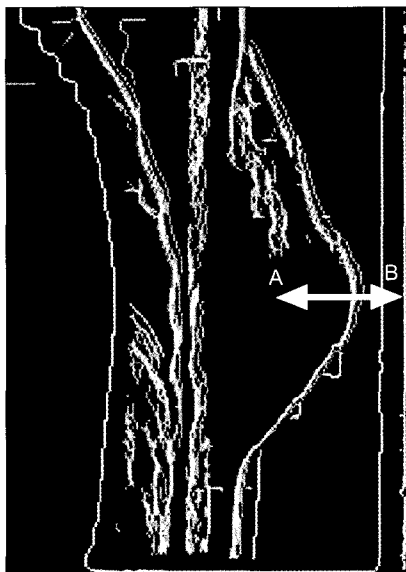


Fig. 4. A cumulative image generated by applying edge detection to trace tissue interfaces (along the lung and skin) and field edges for a set of EPID images. Each image has a pixel value of 0 for background and 1 for outline (edge). Outlined images were combined into a composite image.

tissue-air. The software assigns the image a pixel value of 0 for background, and 1 for detected edges. Outlined images were accumulated into a composite image as shown in Fig. 4. Field corners were used as registration points for superimposing images. This image had the maximum pixel value equal to the number of images where the delineated edges overlapped.

A statistical analysis tool was built into the automated analysis software. Composite images show edges (or outlines) as a spread of lines following a common path. Where the outlines were spread along the chest wall, the in-house software enabled us to draw an analysis line (from point A to B as shown Fig. 4) perpendicular to the tangent at the apex of the breast, and produced the graph (dotted) based on where those lines fell on the analysis line as illustrated in Fig. 5. Once the data has been collected from the composite image, the software creates a Gaussian graph (solid line) representing the composite error, and calculates the standard deviation (σ). The X-axis, "Selected Length", is a relative dimension that depends on where the line started and stopped for measurement and analysis.

2-D compensators are fabricated with a number of alu-

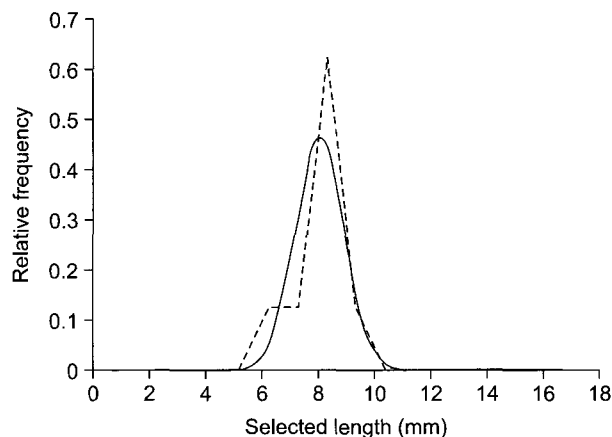


Fig. 5. Gaussian spread (solid line) and standard deviation (σ) (dashed line) based on the cumulative measurement of edges crossing a reference line. The X-axis, Selected Length, is a relative dimension, which depends on where the line started and stopped for measurement and analysis.

minum and copper cubes. Between the cubes there is some leakage, which appears as grids in edge detected images. Lines and dots produced by detector leakage and noise were removed before analysis.

4. Measurement

A total of 2,931 electronic images were taken in cine mode for this study. Twelve patients were filmed and analyzed for intra and interfractional errors. Since beam geometry can affect PTV margins, the range of gantry angles for the patient selection is depicted in Fig. 1 and Fig. 2 for future reference. Intrafractional error was measured with a composite image of cine-mode images for each field during a daily treatment. Fig. 6 shows composite images taken over five consecutive days. The top row presents the medial composite images. Each composite image is assembled from 8 to 9 images. Bottom row images show the composites of the lateral field. The anterior-to-posterior breast motion on the breast mid-plane was tracked at three different locations on the breast: the top 1/3, middle (apex of the breast), and bottom 1/3 of each image.

The standard deviations (SD) measured at each location were averaged for each daily image data set throughout the 7 to 15 treatment days. For each patient, the SD was averaged over the entire span of treatment days. From the SD, the 95% confidence levels ($2 \cdot (1.96 \cdot \sigma)$) were calculated for all patients.¹⁷⁾ The measurement results are summarized in Fig. 7.

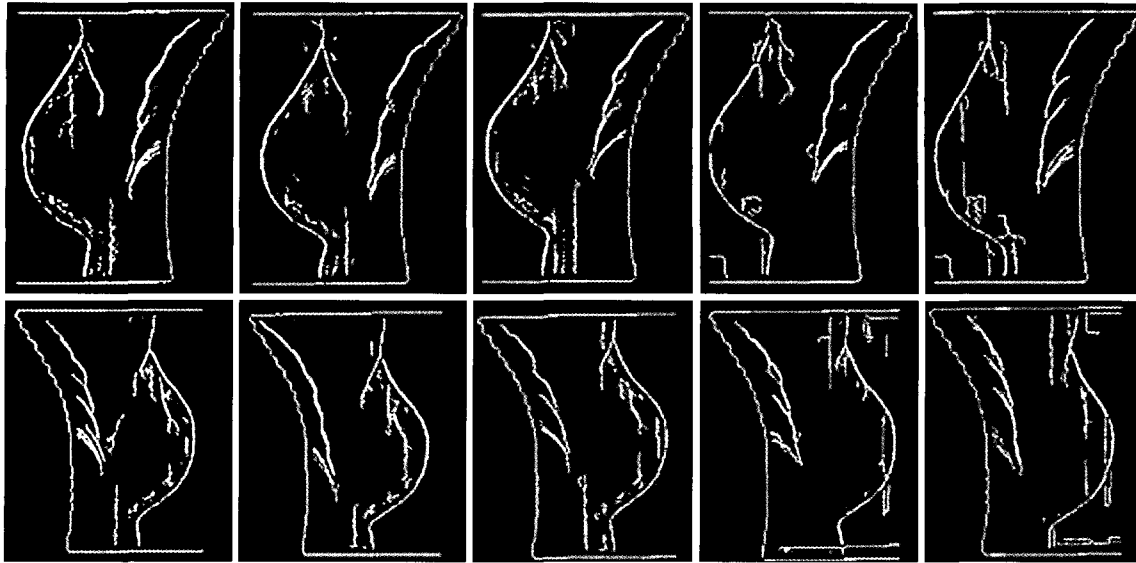


Fig. 6. Intrafractional medial (top) and lateral (bottom) cumulative images covering five consecutive fractions (columns) from Patient 11. Eight to Nine images were taken during single fraction irradiation and processed. Tissue interface edges were detected using the Canny edge detection technique. Edge detected images were registered and overlaid in a frame with a reference line at the medial field edge. These images show nearly identical line spread.

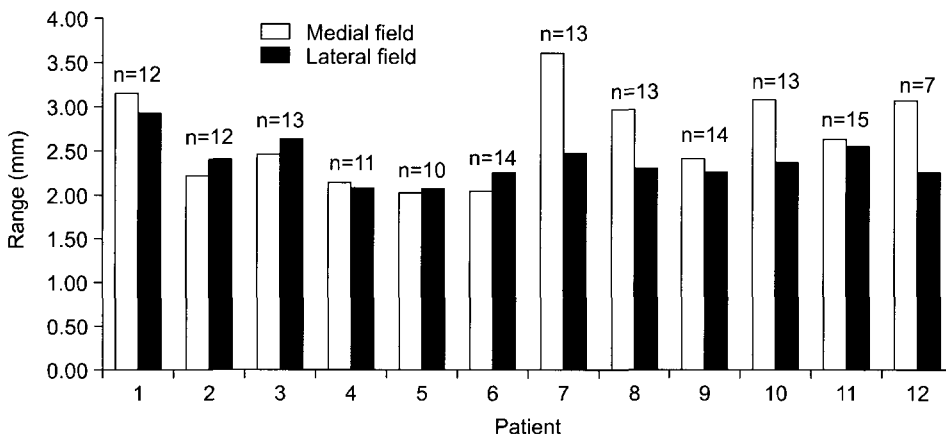


Fig. 7. Intrafractional motion analyses showing eight to nine images per fraction, acquired for 7 to 15 fractions (n). Measurements at 1/3, 1/2, and 2/3 of the vertical image axis in were averaged for each fraction. The 95% confidence values were calculated from composite images.

For the interfractional error analysis, one image from a set of images taken in cine mode per treatment day was randomly selected from the entire treatment set. These randomly selected images were outlined and accumulated into a composite image. An example is shown in Fig. 8. The grid size in the figure is 1 cm by 1 cm.

The anterior-to-posterior breast motion of the breast mid-plane was again tracked at three different locations: top 1/3, middle (apex of the breast), and bottom 1/3 of each image. For each patient, the standard deviations were averaged at

three locations. The 95% confidence levels were calculated and summarized Fig. 9.

RESULTS

The standard deviation from intrafractional motion did not show significant variation among patients as shown in Fig. 7. The 95% confidence level from the intrafractional motion (due mostly to breathing) ranged from 2 mm to 4 mm. Between 12 patients the variation was within 2 mm. The dif-

ference between medial and tangential fields was negligible. For each patient, the intrafractional error was very consistent, showing minor variations between treatment days (a sample analysis is illustrated in Fig. 6). The line spread in each composite image was almost identical for 5 consecutive days. However, the 95% confidence level from the interfractional error (due mainly from daily setup error) ranged from 7 mm to 31 mm shown in Fig. 9. The average of 95% confidence

levels over 12 patients was 17 mm. Fig. 8 shows the interfractional error as an example. The outline spread was much more significant compared to that from intrafractional motion shown in Fig. 6. The variation between patients was obvious and exceeded 15 mm. Some patients showed significant differences between medial and lateral fields, which were larger than 5 mm. This may result from the geometry used for imaging. Since all images were taken at the gantry angle used for treatments, expansion of the chest-wall from breathing may vary in the beam direction and will differ between medial and lateral fields.

Our automated analysis software demonstrated itself to be robust. It took 2 days to analyze approximately 720 measurements (2,931 EPID images). We found the automatic functionality was very useful to process the large number of images required for a statistically meaningful characterization of a clinical modality.

DISCUSSION AND CONCLUSIONS

The 95% confidence values of intrafractional motion ranged from 2 to 4 mm on 12 patients. However, the interfractional setup error, which ranged from 7 mm to 31 mm, was significantly larger than patient breathing motion. Some breathing motion is folded into the interfractional error depending on what moment during the breathing cycle the image was taken. However, the magnitude of interfractional error compared to intrafractional error indicates that breathing motion is not a significant contributor to the former. The random se-

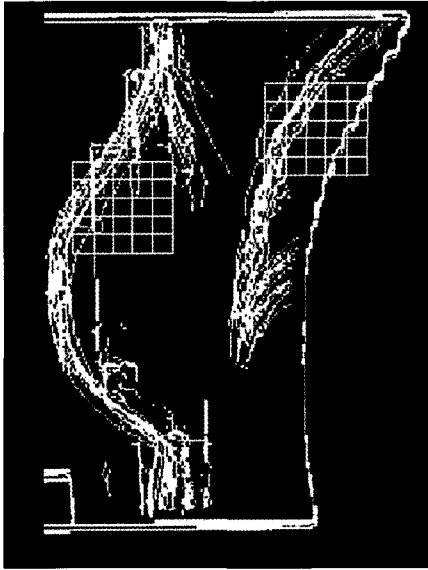


Fig. 8. An Interfractional analysis image is generated by randomly selecting one image from each of 17 fractions and accumulating them into a single image. This composite of medial images shows how much interfractional setup error occurs in addition to breathing motion. A 1×1 cm grid is provided for reference.

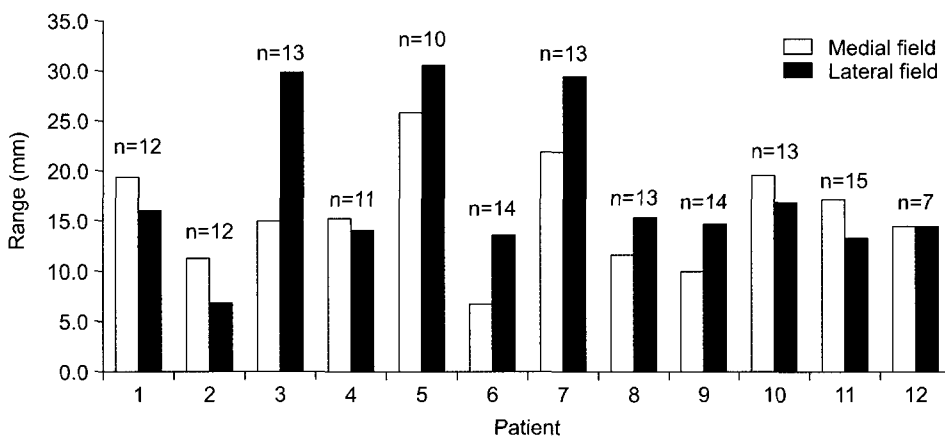


Fig. 9. A summation of interfractional patient movement. One image per fraction was randomly chosen through breathing cycle (s). The number of fractions sampled ranged from 7 to 15 for twelve patients. Measurements at 1/3, 1/2, and 2/3 of the vertical image axis in were performed. From the measurements, the 95% confidence values were calculated.

lection of the images probably helps in minimizing this effect. Since there was little variation among patients, breathing motion results from this study can be applied to the general patient population unless a particular patient's lung capacity deviates significantly from the average. Daily setup error may vary depending on the technique used for patient setup (and what institution-specific immobilization device may be in use). Prior to 3-D conformal radiation treatment or IMRT delivery to breast patients, the magnitude of setup error must be measured and properly formulated into the PTV. To reduce large PTVs, a setup verification device may be required for breast IMRT or 3-D CRT. Commercial software that comes with EPIDs typically analyzes only single images and does not provide edge detection. Automated analysis software is very helpful to process the large number of EPID images required to characterize a particular treatment and formulate a PTV. It can provide us valuable information with minimal effort.

It should be noted, that to fully characterize a treatment PTV, positional accuracy examined in this study is not wholly sufficient. The usefulness of a PTV depends on accurate CTV delineation. Target accuracy (accurate CTVs) will be an important factor for 3D conformal fields as is indicated by current issues in defining the CTV for electron boost fields. The commonly used clinical technique to define an electron boost field is based on the resection scar and palpating the tumor bed. If the bed is palpable, a 1 cm margin was added. If it is not, then a 3~4 cm margin was placed parallel to the surgical scar. Benda et al. compared the commonly used clinical technique to an approach based on CT imaging of surgical clips in tumor beds.¹⁸⁾ In their proposed technique, the CTV was contoured with the surgical clips as a guide but also incorporated any surgical defect or seromas seen on the CT scans. For daily setup error and organ motion, the PTV was created with a 1 cm margin added to the CTV. Their results showed that the isocenter differed more than 1 cm in the medial-lateral direction in 5 of 30 patients and in the cephalocaudal direction in 12 of 30 patients. Clearly, our findings on PTV derivation must follow a carefully delineated CTV for 3D conformal or IMRT breast treatment.

Our images were taken at the treatment beam gantry angles with treatment apertures. Therefore, our specific PTV margins should only be applied to tangential beam arrangements

acquired in that particular clinic. However, our findings can be used as a minimum margin to compensate for daily setup error and breathing motion. To further reduce margins, an image-guided system is recommended for patient position verification. Our automated EPID analysis can be extended to other treatments by acquiring digital images specific to that treatment geometry.

REFERENCES

1. ICRU 50: *Prescribing, Recording, and Reporting Photon Beam Therapy*. International Commission on Radiation Units and Measurements, 1993.
2. Fein DA, McGee KP, Schultheiss TE, Fowble BL, Hanks GE: Intra- and interfractional reproducibility of tangential breast fields: a prospective on-line portal imaging study. *Int J Radiat Oncol Biol Phys* 34(3):733-740 (1996)
3. Baroni G, Garibaldi C, Scabini M, et al: Dosimetric effects within target and organs at risk of interfractional patient mispositioning in left breast cancer radiotherapy. *Int J Radiat Oncol Biol Phys* 59:861-871 (2004)
4. George R, Keall PJ, Kini VR, et al: Quantifying the effect of intrafraction motion during breast IMRT planning and dose delivery. *Med Phys* 30:552-562 (2003)
5. Hector CL, Evans PM, Webb S: The dosimetric consequences of inter-fractional patient movement on three classes of intensity-modulated delivery techniques in breast radiotherapy. *Radiother Oncol* 59:281-291 (2001)
6. Hurkmans CW, Remeijer P, Lebesque JV, Mijnheer BJ: Set-up verification using portal imaging; review of current clinical practice. *Radiother Oncol* 58:105-120 (2001)
7. Lirette A, Pouliot J, Aubin M, Larochelle M: The role of electronic portal imaging in tangential breast irradiation: a prospective study. *Radiother Oncol* 37(3):241-245 (1995)
8. McGee KP, Fein DA, Hanlon AL, Schultheiss TE, Fowble BL: The value of setup portal films as an estimate of a patient's position throughout fractionated tangential breast irradiation: an on-line study. *Int J Radiat Oncol Biol Phys* 37(1):223-228 (1997)
9. Pouliot J, Lirette A: Verification and correction of setup deviations in tangential breast irradiation using EPID: gain versus workload. *Med Phys* 23(8):1393-1398 (1996)
10. Canny J: A computational approach to edge detection. *IEEE Trans. Pattern Anal Mach Intell* 8(6):679-698 (1986)
11. Nalwa VS, Binford TO: On detecting edges. *IEEE Trans. Pattern Anal Mach Intell* PAMI-8:699-714 (1986)
12. Sarkar S, Boyer KL: Optimal infinite impulse response zero crossing based edge detectors. *CVGIP: Image Understanding* 54:224-243 (1991)
13. Sobel I: *An isotropic 3x3 Image Gradient Operator*. Machine Vision for Three-Dimensional Scenes: Academic Press, 1990 pp. 376-379
14. Ding L, Goshtasby A: On the Canny edge detector. *Pattern*

Recognition 34:721-725 (2001)

15. Heath M, Sarkar S, Sanocki T, Bowyer K: Comparison of edge detectors. Computer vision and image understanding, 69(1):38-54 (1998)

16. Ellis F, Lescrenier C: Combined compensation for contours and heterogeneity. Radiology 106(1):191-194 (1973)

17. Zwillinger D. *Standard Mathematical Tables and Formulae*. CRC Press, Inc., Troy, New York (1996), pp. 639

18. Benda RK, Yasuda G, Sethi A, Gabram S, Hinerman RW, Mendenhall NP: Breast boost: Are we missing the target? Cancer 97:905-909 (2003)

유방암 방사선치료에 있어 치료도중 및 분할치료 간 위치오차에 대한 전자포탈영상의 컴퓨터를 이용한 자동 분석

*Department of Radiation Oncology, Ireland Cancer Center, Case Western Reserve University School of Medicine, Cleveland, †Department of Radiation Oncology, Mallinckrodt Institute of Radiology, Washington University School of Medicine, St. Louis, ‡Department of Radiation Oncology, University of Florida College of Medicine, Gainesville, §가톨릭대학교 의과대학 의공학교실

Jason W. Sohn*, David B. Mansur†, James I. Monroe*, Robert E. Drzymala†, 진호상‡, 서태석§, James F. Dempsey‡, Eric E. Klein†

유방암 환자의 방사선치료에 있어 치료도중(intrafractional) 및 분할 치료 간(interfractional)에 발생하는 오차를 측정하는 자동분석소프트웨어를 개발하였다. 오차 분석 결과는 3차원 입체조형 방사선치료를 임상에 적용하기에 앞서 적절한 치료 계획용적(Planning Target Volume, PTV)을 설정하는 데 있어 매우 중요하다. 본 연구에서는 전자포탈영상장치(Electrical Portal Imaging Device, EPID)로써 Portal Vision LC250 액체 충전형 이온화 검출기를 사용하였다(fast frame-averaging 모드, 초당 1.4 프레임, 256×256 픽셀). 12명의 환자에 대해 최소 7일 이상씩 영상을 획득하였다. 매 치료마다 평균 8 내지 9개의 영상을 각 빔에 대해 얻었다(분당 400 MU 선량률). 총 2,931 (720 측정을 포함하는)개의 영상을 정량적으로 분석할 수 있는 자동화 영상 분석 소프트웨어를 개발하였다. 이를 통해 호흡으로 인해 발생하는 치료도중 오차와 분할 치료간 발생하는 분할치료오차의 표준편차(σ)들을 계산하였다. 신뢰구간 95%로 임상표적체적(Clinical Target Volume, CTV)을 포함할 수 있는 PTV 마진은 $2 \cdot (1.96 \cdot \sigma)$ 으로 계산되었다. 주로 호흡으로 인해 유발되는 치료도중오차를 보상하기 위해 필요한 PTV 마진은 2 mm에서 4 mm이었다. 반면에 분할 치료간 오차를 보상하기 위해 필요한 PTV 마진은 7 mm에서 31 mm이었다. 12명의 환자에 대한 전체 평균오차는 17 mm이었다. 분할치료 간 오차는 호흡에 의해 유발되는 치료도중 오차에 비해 2배에서 15배까지 더 크게 나타났다. 유방암 치료에 있어 3차원 입체정형조사나 세기조절방사선치료(Intensity Modulated Radiation Therapy, IMRT)를 적용하기에 앞서 반드시 셋업 오차의 크기를 측정하여 PTV에 적절히 반영되어야 한다. 유방에 대한 3차원 입체정형조사나 세기조절방사선치료를 위해 반드시 필요한 것은 아니지만, 큰 PTV 마진을 줄여주기 위해서는 영상유도방사선치료(Image Guided Radiation Therapy, IGRT)가 매우 유용하게 이용될 수 있다. 전자포탈영상장치 들은 본 보고서에서 기술한 바와 같은 자동분석소프트웨어를 반드시 포함하여야 한다. 이를 통해 수많은 EPID 영상들을 자동화 처리하고 오차분석을 시행함으로써 각 병원의 임상적용 방법 및 환경에 따라 상이하게 나타날 수 있는 오차의 크기를 감안한 적절한 PTV마진을 구하는데 도움을 얻을 수 있다. 이러한 장치들은 또한 최소의 노력으로 환자 치료를 관찰할 수 있는 귀중한 정보를 제공해 준다.

중심단어 : 전자포탈영상장치, 유방, Canny 경계선 검출, 방사선 치료, 위치 오차